Remote sensing vs. field survey data in a post-earthquake context: Potentialities and limits of damaged building assessment datasets

Daniel Monfort, Caterina Negulescu, Myriam Belvaux

▶ **To cite this version:**

Daniel Monfort, Caterina Negulescu, Myriam Belvaux. Remote sensing vs. field survey data in a post-earthquake context: Potentialities and limits of damaged building assessment datasets. Remote Sensing Applications: Society and Environment, 2019, 14, pp.46-59. 10.1016/j.rsase.2019.02.003 . hal-02053131

HAL Id: hal-02053131
https://brgm.hal.science/hal-02053131

Submitted on 22 Oct 2021

HAL is a multi-disciplinary open access archive for the deposit and dissemination of scientific research documents, whether they are published or not. The documents may come from teaching and research institutions in France or abroad, or from public or private research centers.

L'archive ouverte pluridisciplinaire **HAL**, est destinée au dépôt et à la diffusion de documents scientifiques de niveau recherche, publiés ou non, émanant des établissements d'enseignement et de recherche français ou étrangers, des laboratoires publics ou privés.

Distributed under a Creative Commons Attribution - NonCommercial 4.0 International License

Version of Record: https://www.sciencedirect.com/science/article/pii/S2352938518303161
Manuscript_226999784c22e9fea7707e38143707e1

Remote sensing vs. field survey data in a post-earthquake context: potentialities and limits of damaged building assessment datasets

Authors:

D. Monfort, C. Negulescu and M. Belvaux

Keywords

Seismic risk, vulnerability, remote sensing, damage assessment

Abstract

Quick building damage assessment following disasters such as large earthquakes serves to establish a preliminary estimation of losses and casualties. These datasets are completed by employing several crowdsourcing initiatives, in which volunteers and collaborators map damaged buildings in a given area at a qualitative damage scale based on a post-earthquake aerial or satellite image. Automating this process is a temptation and a technical issue, but manual interpretation remains essential, with the identification of moderate and lateral damage being the key and limiting factor. Following the Haiti 2010 earthquake, many studies were completed by crossing multilayer data gathered from different sources (satellite, aerial, and field survey). These works created a building damage dataset that enabled the construction of different sets of empirical vulnerability functions. In the present study, we proposed to review the datasets used for the damage assessment again, investigate how they can be managed for understanding urban damage patterns, and quantify the potentialities and limits of the sets.

A high-resolution map of damage in Port-au-Prince was used to obtain a deducted map of intensity and was then compared to more detailed post-earthquake investigations such as the microzonation of the city (Belvaux et al. 2018). These detailed post-earthquake investigations, in which array microtremor measurements are performed for characterization of the subsurface soil, contribute to a better understanding of local variations in intensity. Subsequently, a retro damage scenario was run, considering the different sets of vulnerability functions (using the RISK-UE methodology vulnerability indexes) fitted with empirical vulnerability functions. Using the characterization of the exposure on a remote sensing basis, the results fit the heaviest damage well (building collapse), but they overestimated moderate damage states compared to the observations. However, is an aerial image based dataset sufficiently exhaustive for moderate damage, which is mostly visible from a lateral or internal point of view? Finally, we suggested some range of adjustments that can be applied to a vulnerability assessment originating from remote sensing data such that it can be used more accurately in the detection of urban damage, even for moderate damage degrees.

© 2019 published by Elsevier. This manuscript is made available under the CC BY NC user license
https://creativecommons.org/licenses/by-nc/4.0/

1. Introduction

Several rapid mapping initiatives utilized post-earthquake satellite and airborne imagery to produce independent point feature sets marking the damage grade of affected buildings (such as the European program Copernicus Emergency Management Service and HOT from the Open Street Map community). Despite the obvious potential of satellite remote sensing technology in providing damage figures, the scale and complexity of the urban structures caused the overall figures and patterns of the damage assessments to yield a rather poor representation of the true damage extent.

The higher detail airborne imagery performs much better as confirmed by different validation studies conducted during the last several years (Saito et al. 2010; Corbane et al. 2010; Ghosh et al. 2011; Lemoine and Corbane 2013). (Lemoine and Corbane 2013) investigated the quality of damage assessments derived from different activities such as, satellite-based damage assessments, aerial-based damage assessments, field survey following a stratified random sampling, road track surveys from a Low Cost Mobile Mapping System, and block-sampling using Pictometry data, through a simple intercomparison and a validation using a complete building ground survey. The results showed that the identification of building damage from aerial imagery provides a realistic estimate of the spatial pattern and intensity of building damage, even if it still tends to underestimate several damage states that are difficult to effectively identify from an aerial point of view. (Dong and Shan 2013) completed a review work of pre- and post-earthquake damage assessment, and assessed what remote sensing techniques, optical or not, are the most used in these cases: LIDAR, SAR, optical image, and ancillary data. Even if techniques such as LIDAR have serious benefits (as for example to estimate debris volume), they found that optical images, satellite or aerial, remain the most reliable and independent evaluation. More recently, (Cooner, Shao, and Campbell 2016) presented a work testing three algorithms to automatically map post-earthquake damage based on machine learning methods with great results. However, they provided results in a binary form: damaged and undamaged, based on the most easily visible damage (total collapse). (Romaniello et al. 2017) provides damage in terms of collapse ratio with automatic image processing using Haiti 2010 Earthquake dataset. Remote-sensing-derived data is also a prevention tool to estimate built-up areas and exposure to natural hazards such as earthquakes (Ehrlich et al. 2018). Remote sensing can be used during all the phases of natural risk management (prevention, preparedness, crisis management, recovery, and reconstruction).

The January 12, 2010, Port-au-Prince Earthquake in Haiti (M7-7.1) killed more than 200,000 people (Calais et al. 2010). It was felt in all Hispaniola Island (Haiti and Dominican Republic) and in the East part of Cuba. It was the first earthquake with an important work completed by several international organizations generating a building damage dataset in the Port-au-Prince area. The goal of this work was to estimate as soon as possible an order of magnitude of the damaged buildings and its economic impact for international donors. Therefore, in more recent earthquakes such as Amatrice in Italy, Ecuador, and Nepal in 2016, remote sensing has been used to aid damage assessment (Karimzadeh and Mastuoka 2017; Piscini et al. 2017; Copernicus EMS 2016; Copernicus 2015).

However, other potential uses of these datasets exist, such as the establishment of empirical vulnerability curves for Caribbean countries' building types. A very important work regarding the identification and cartography of damaged buildings was attempted for the 2010 Haiti Earthquake using several techniques for identification of the damaged areas and structures (remote sensing, aerial images, field inventory, etc.). Based on these databases, some authors have proposed empirical fragility functions adapted to current Haitian buildings (Hancilar, Taucer, and Corbane 2010; Hancilar, Taucer, and Corbane 2013; Molina et al. 2014). In another context, South American countries, (Villar-Vega and Silva 2017) run retro damage scenario for several past events and compared it with building damage datasets, in terms of collapsed buildings. They used a set of fragility curves representative of these countries, but they did not adapt a new set of curves. Among the main limitations they observed was the variation in the

portfolio when comparing models, based on recent census data, with past events 15 years old and the quality and heterogeneities (in terms of damage states) among the building damage datasets.

The present work discusses these previous works in damage and vulnerability assessment completed after the 2010 earthquake and proposes a high-resolution intensity map based on observed damage in the Port-au-Prince area. This map was compared to the USGS ShakeMap (USGS 2017), which was calculated during the hours/days after the earthquake, and some authors consider it as the reference in terms of the intensity for this event. However, it should be considered that for this event, in reality, there were very few observed or measured data considered in the ShakeMap calculation. Consequently, ShakeMap for this event was mostly a model obtained using a ground motion prediction equation (GMPE) calculation.

During the following years after the earthquake, important works have been completed in Haiti to better understand this earthquake and its effects. (Rathje et al. 2011) compares building damage patterns with available geological units, topographic units and identifies damage pockets. In terms of lithological site affecting the seismic microzonation in Port-au-Prince, studies have been completed (Bertil et al. 2015; Belvaux et al. 2018). The fault delimitation and its characterization (Calais et al. 2010) and the most appropriate GMPE for a Haitian context have been proposed (Molina et al. 2014; Torres et al. 2016). Considering all this information, the intensity of the 2010 earthquake can also be simulated.

Consequently, three intensity maps were compared in the present work: the USGS ShakeMap calculated during the first hours/days, an intensity map derived from the observed damage database (JRC database), and a simulated intensity map considering new investigations completed after the event: lithological site effects, fault characteristics, and most adapted attenuation relation.

Finally, we ran several retro-damage scenarios, considering appropriate fragility functions for the typical Haitian building stock and the aforementioned three intensity maps in the Port-au-Prince municipality.

2. Remote sensing and post-earthquake damage assessment

Following the Port-au-Prince earthquake, several actions and works were completed to assess the damage and habitability in the area as soon as possible. Among them, the most important was a joint collaboration between the United Nations Institute for Training and Research (UNITAR), the Operational Satellite Applications Programme (UNOSAT), European Commission Joint Research Centre (EC JRC) and the World Bank ((UNITAR/UNOSAT 2010), referred as UWJ hereafter. In fact, many institutions and volunteers collaborated during the weeks following the earthquake to produce a final global building damage assessment for the Port-au-Prince area (11 municipalities). Given its huge volume of data in the most impacted area, this dataset is the reference in terms of damage assessment for the 2010 earthquake.

Based on this work, several UWJ authors (Corbane et al. 2010; Ghosh et al. 2011; Lemoine and Corbane 2013;) compared damage building datasets after the Port-au-Prince Earthquake. Ghosh et al. (2011) presented a work completed by the GEO-CAN[1] damage assessment, in the framework of joint collaboration, which produced a damage building dataset combining satellite images, aerial images, fieldtrip validations in some zones and even some data estimated by models. The EMS98 damage scale was used as shown on Figure 1. The authors have validated this data by field trip in several districts. They have worked with pre-earthquake images, noting each pre-existing building. They compared it to the Open Street Map (OSM) and Chinese Academy of Sciences (CAS) quick damage assessment using satellite images, in which only collapsed buildings were identified. As occurred in other recent

[1] Global Earth Observation Catastrophe Assessment Network

earthquakes, crossing aerial estimation with field trip observations, they found that the main difficulty was identifying the partial collapses and intermediate-moderate damage states.

Another important dataset of damages is the MTPTC dataset (Haitian Ministry of Public Works and Telecommunications) created by Miyamoto et al. (2011), which contains household habitability (classified using a color code: green, yellow, or red) and % of loss. It is based on fieldtrip work, using the USA ATC-20 method to assess habitability. Their work was completed building by building.

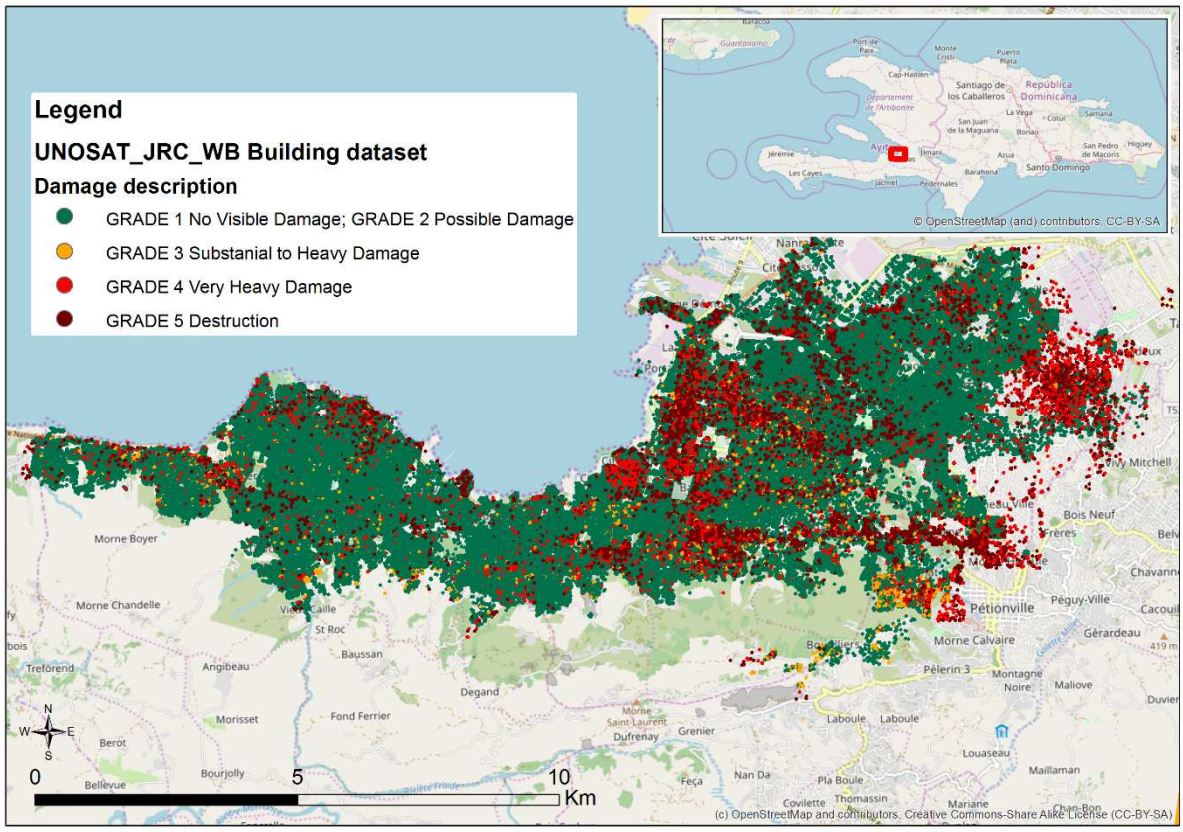

Figure 1: UNOSAT-JRC-WB damage dataset of Port-au-Prince and surroundings area. Basemap OSM.

Globally, the MTPTC and UWJ datasets are quite coherent in total sum. However, great differences can be found in several areas, as is noted by Lemoine and Corbane (2013); in completely destroyed areas, the MTPTC could underestimate the number of initial buildings. The MTPTC survey's main goal was to assess damage in remaining buildings. In addition to the complexity in assessing damage degree, another difficulty is comparing habitability surveys, which mix structural and functional points of view (such as the MTPTC survey) with damage degree surveys (such as UWJ) which are mostly structural. (Douglas et al. 2015) found the same type of difficulties in the L'Aquila earthquake datasets.

(Saito et al. 2010) using the Pictometry methodology, assessed 1300 buildings in the Port-au-Prince area. Pictometry® is the name of a patented aerial image capturing process that produces imagery showing the fronts and sides of buildings and locations on the ground (EagleView, n.d.). They have compared observed damage to an intensity MMI map (ShakeMap) completed by the US Geological Survey (USGS) but they did not identify a clear relation. In their opinion the whole area of Port-au-Prince should be classed as MMI=IX. They analyzed the reasons for the great differences between the damage assessment completed using GEO-CAN (using satellite imagery) and that using Pictometry. GEO-CAN is not exhaustive in delimiting pre-existing buildings and cannot correctly identify intermediate damage, mostly the identification of the D4 EMS98 damage state (partial collapse). They

also compared their results to a field survey damage assessment of only 124 buildings; even with a better view of lateral damage obtained using Pictometry (soft story, moderate damage), damage was still underestimated using Pictometry. Looking at some of the individual buildings, the principal causes of these discrepancies were lower-story collapses, which were not visible in Pictometry, and cases where the Pictometry image was obscured by either trees or adjacent buildings. The main limit of this comparison is the reduced number of buildings assessed in the field.

Table 1: Synthesis of damage observations in the Port-au-Prince area completed by different authors.

Data source	Method	Area /specifications	Assessed buildings	% buildings D4 and D5
UWJ dataset	Aerial images + fieldwork validation in several areas	Shanty zones, Port-au-Prince municipality	40,270	23.6
		Residential low-medium-high density, Port-au-Prince municipality	50,100	25.15%
GEO-CAN	Hybrid methodology: Satellite images, field surveys, and modelled data	Whole Port-au-Prince area, 11 municipalities	298,739	19.6%
		Port-au-Prince municipality	106,902	23.5%
MTPTC (Miyamoto et al. 2011)	Fieldwork Habitability using ATC-20 assessment	Single-family	290,381	21% (red color tag)
		Multifamily	70,175	16% (red color tag)
(Cambridge Architectural Research Ltd 2010; Saito et al. 2010)	Pictometry	Downtown	199	28.2%
		Residential	308	19.15%
		Shanty	354	21.75%
EEFIT (Saito et al. 2010)	Fieldwork	8 different locations	142	46%

3. Data interpretation

3.1. Deducted intensity maps of Port-au-Prince following the 2010 earthquake

Seismic intensity for the 2010 earthquake has been characterized using very poor data. (Hough, Taniguchi, and Altidor 2012) and (Gould et al. 2011) proposed PGA and intensity values at several points in Port-au-Prince based on damage assessment of very specific structure and electrical equipment. As a consequence of this poor data, the construction of empirical vulnerability functions has to address semi-modelled intensity data, as was completed by (Ufuk Hancilar, Taucer, and Corbane 2013) who proposed empirical vulnerability functions (in PGA, PGV, and intensity) based on the USGS ShakeMap

for this event. ShakeMap is a calculation combining observed (seismic stations and intensities) and modelled data (ground motion prediction equation). However, the first versions of the 2010 earthquake's ShakeMap were simply a model of ground motion via attenuation relations, fitted only by several Do you feel it (DYFIT) points from web intensity forms from the USGS website. More recently, the USGS has produced a new version of the intensity and PGA ShakeMap of the 2010 Earthquake, integrating more DYFIT points than previous versions. In both cases, the intensity in the Port-au-Prince municipality was approximately VIII MMI.

However, as previously discussed, the damage assessment is very comprehensive and exhaustive (locating every building) in urban areas combining field surveys, aerial images and satellite information. Instead of using models to estimate macroseismic intensity such as ShakeMap fitted with several sparse observations (DYFIT), in this work we propos to obtain a high-resolution macroseismic intensity map of Port-au-Prince based on damage assessment.

The EMS98 scale was used in this work (Conseil de l'Europe 1998). The Port-au-Prince area (covered by the UWJ damage assessment) was divided into grid cells 500 m in length. For each cell, an intensity value was estimated based on the damaged building, the total number of buildings was counted, and their damage distribution was calculated (buildings in damage states D5, D4, D3, and no visible-slight structural damages). To be as representative as possible, cells with less than 10 buildings and cells with only completely destroyed buildings were not considered.

A work has been completed to clearly identify the areas where the UWJ dataset is exhaustive or not using slightly damaged buildings. In some areas, only buildings in the D4 and D5 state exist on the UWJ dataset while many more buildings occur; this means that in these areas UWJ only identified heavily damaged buildings. Regardless, this situation is quite rare within the Port-au-Prince municipality.

The EMS98 scale considers six vulnerability classes of buildings. Globally, all of the buildings in the area are considered as vulnerability class B (Grunthal and Levret 1998). This means that all of the buildings correspond to reinforced concrete (RC) structures with no seismic design or unreinforced masonry buildings. The most vulnerable class in EMS98 (A) does not represent the whole building typology in Haiti (no adobe or stone masonry buildings occur in Haiti). This choice has a major impact in the intensity evaluation. Consequently, the intensity was deducted as in Table 2 (Giovinazzi 2005; Milutinovic and Trendafiloski 2003). Following this table, for each regular cell, three estimations of intensity values were done, according to the three damage degrees. It is possible that two different intensities (or three) are deducted for each damage state. Intermediate values (such as 9.5) are attributed in this case.

Table 2 : Relation between damaged percentage in one cell and EMS98 intensity for buildings in vulnerability class B (Milutinovic and Trendafiloski 2003; Giovinazzi 2005)

EMS98 intensity in cell i	% of buildings in cell in D5		
		D4	D3
XI	>50%		
X	10-50%		
IX	0-10%	>10%	
VIII		0-10%	10-50%
VII			0-10%

Figure 2 shows a close-up image of an area in Port-au-Prince, showing the damage assessment (color dots) and the estimated intensity. Regular cells where the red and garnet dots are more frequent appear

in intensity IX, cells where buildings in the D4 and D5 states are more scattered in intensity VIII. It is clear that for local differences in terms of damage, the distinction of one degree of intensity at this scale can be justified. The heaviest damage is more concentrated in the southern area.

Figure 2: Close-up image of one district of Port-au-Prince. The back color represents the deducted intensity. The dots represent the damaged buildings from the UWJ dataset.

The obtained intensity in Carrefour, Port-au-Prince, Pétionville, and the Delmas area varies between VIII and X (Figure 3). These intensities are of the same order of magnitude of the values proposed by (Cambridge Architectural Research Ltd 2010) for Port-au-Prince (VIII-IX). The intensity evaluation completed by the USGS with the Internet forms “Do you feel it?” shows VIII at several points in the Port-au-Prince municipality and locally IX in Pétionville.

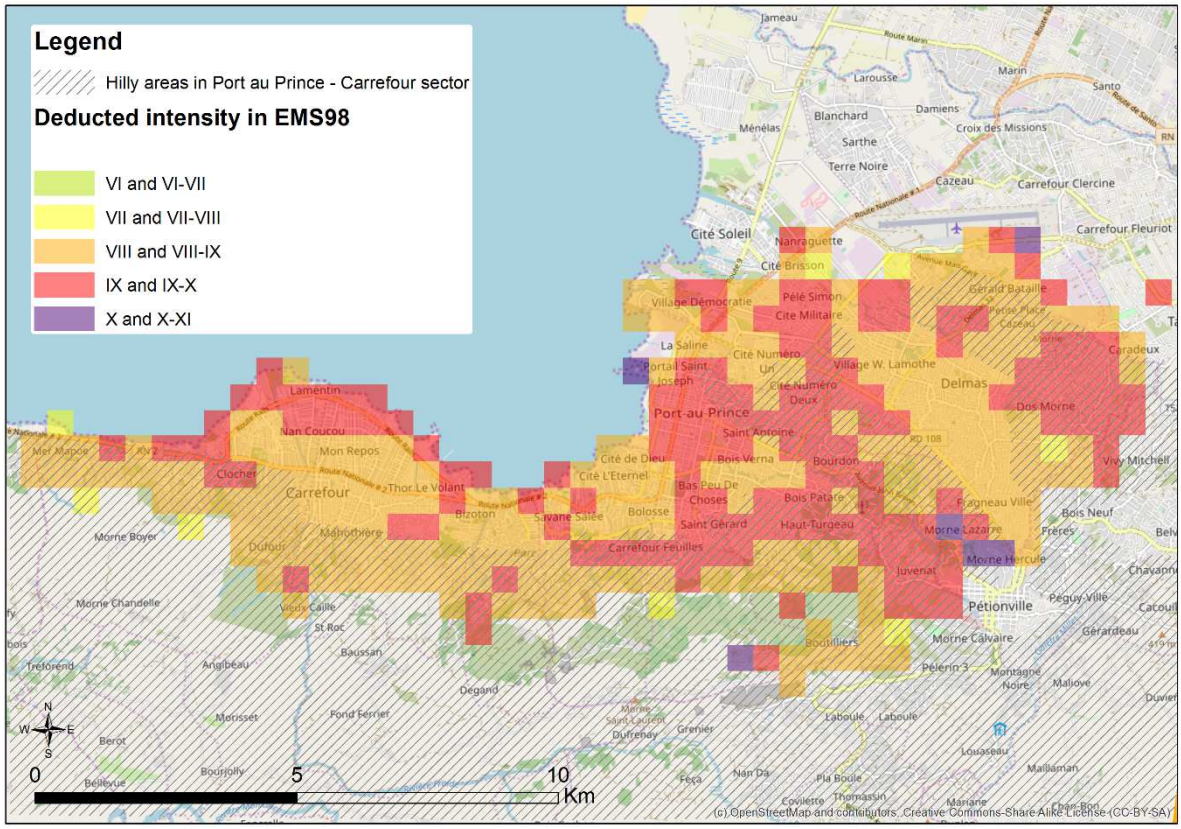

Figure 3: Deducted intensity map, based on the building damage dataset from UWJ in the Port-au-Prince area.

Figure 4 shows a comparison of the obtained intensity map to the USGS ShakeMap, which is the intensity reference map for this event as discussed. Comparing the two intensity maps, the ShakeMap intensities are lower. This is because ShakeMap calculated for several hours after the mainshock for this event considering mostly ground motion attenuation (there are few seismic stations in the area) and the lithological site effects are very summarily considered. Several persons provided punctual damage observations (DYFIT) but the ShakeMap intensity map remains a map with very few/poor data in the Port-au-Prince area. The Eastern part of the studied area (Delmas, Petionville) has intensity values near VIII in ShakeMap but the damage pattern in these areas corresponds to intensity IX or more. To the West (Carrefour), closest to the epicenter, the intensity values in ShakeMap are greater than those obtained using damage. Differences could also be because of the two intensity scales, MMI and EMS98, even if several authors consider that they are equivalent (Musson, Grünthal, and Stucchi 2010).Considering a single vulnerability class, EMS98 and MMI should be close.

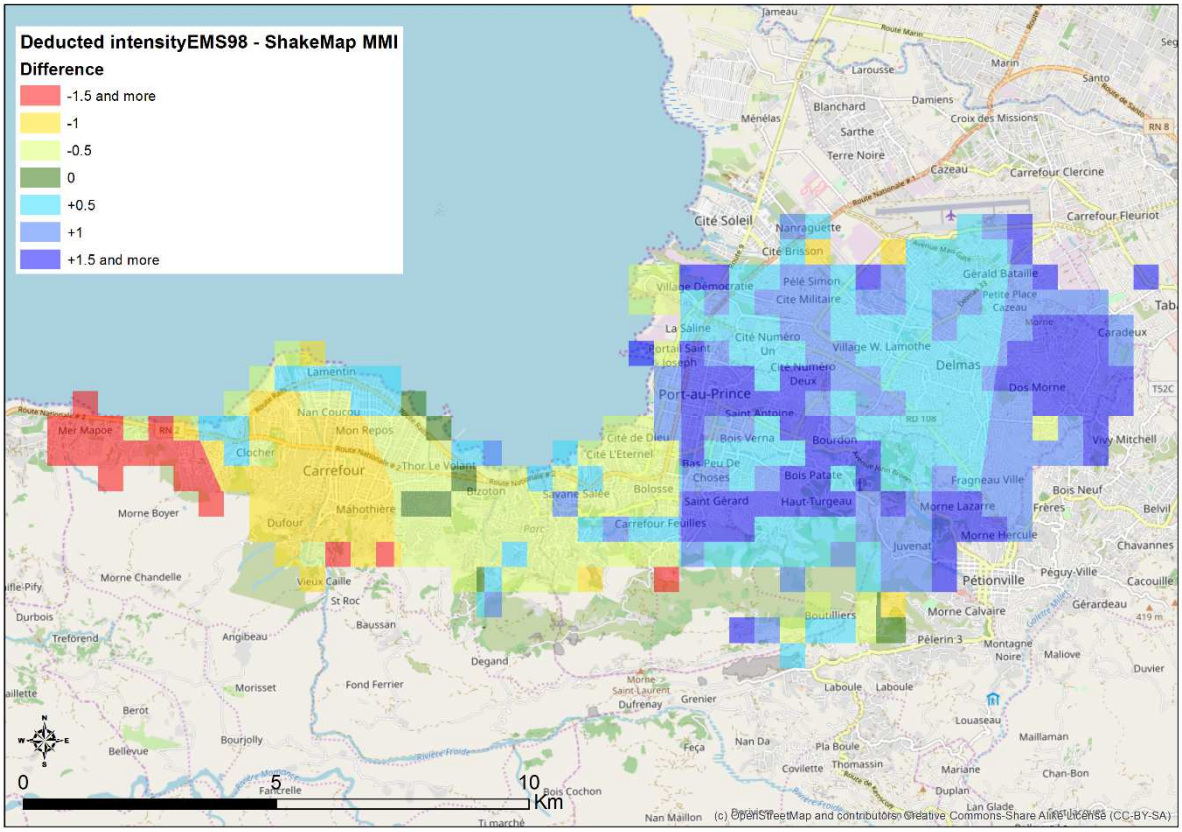

Figure 4: Differences between deducted intensity and the intensity map from the USGS ShakeMap.

3.2. Modelling the intensity using post-earthquake investigations

USGS ShakeMap calculated the intensity map for the Port-au-Prince earthquake during the first hour and then it was updated during the following days after the main shock, integrating the very poor local observed or measured data. Many research works completed during the years after the disaster in Haiti have more knowledge in terms of characterization of the source and the site effects. Therefore, it was important to investigate what the 2010 Earthquake ShakeMap would reveal after being integrated with this new data.

In the present work, we proposed to calculate the 2010 earthquake's intensity map integrating several investigations completed after the earthquake. The steps were as follows: i) estimation of the bedrock PGA choosing the most adequate GMPE for the Port-au-Prince earthquake, the fault location, and the most appropriate magnitude; ii) estimation of the local PGA considering the lithological site effect (microzonation, (Bertil et al. 2015)); and iii) conversion of PGA into macroseismic intensity using empirical relationships. Table 3 summarizes all these parameters.

(Molina et al. 2014) and Torres et al. (2015) proposed the most appropriate GMPE for the Port-au-Prince earthquake (Chiou and Youngs 2008) used for rock conditions. The fault dimension and characteristics were taken from (Calais et al. 2010). Following the earthquake in Haiti, a large seismic microzonation (MZ) project was completed in in the Port-au-Prince area (Bertil et al. 2015; Belvaux et al. 2018). This project characterized and mapped the main geotechnical units in Port-au-Prince (for example, in terms of NEHRP soil classes) (BSSC 2003) as shown in Figure 5. An amplification factor NEHRP was associated with each geotechnical unit as shown in the figure. The Figure 6 presents the intensity map obtained with CY2008 MZ simulation.

GMPE and earthquake parameters	(Chiou and Youngs 2008) for strike slip
	Mw 7.0–7.1 (Calais et al. 2010)
	Top rupture depth 3 km
	Fault delimitation from (Calais et al. 2010)
Soil amplification map and coefficients	(Bertil et al. 2015; Belvaux et al. 2018)
PGA-intensity conversion	(Atkinson and Sonley 2000)

Table 3 : Main characteristics of the simulation termed CY2008 MZ.

Figure 7 shows the differences between the deducted intensity and estimated intensity (CY2008 MZ) and Figure 8 shows it in a map. In the majority of the cells the two values of intensity are equivalent, which is a positive result. In other cases, the intensity is overestimated or underestimated by ½ intensity level, which can be considered acceptable when addressing macroseismic intensity uncertainty. The CY2008 MZ simulation seems to considerably underestimate the intensity (1 intensity level or more) in several cells, mostly in the eastern part of the area. This can be explained by other phenomena not considered here, such as landslides or topographical amplification, and by the ground movement attenuation calculated by the GMPE. (Hough, Taniguchi, and Altidor 2012) showed how overestimated damage areas corresponded with topographical amplification as, for example, in the Petionville area.

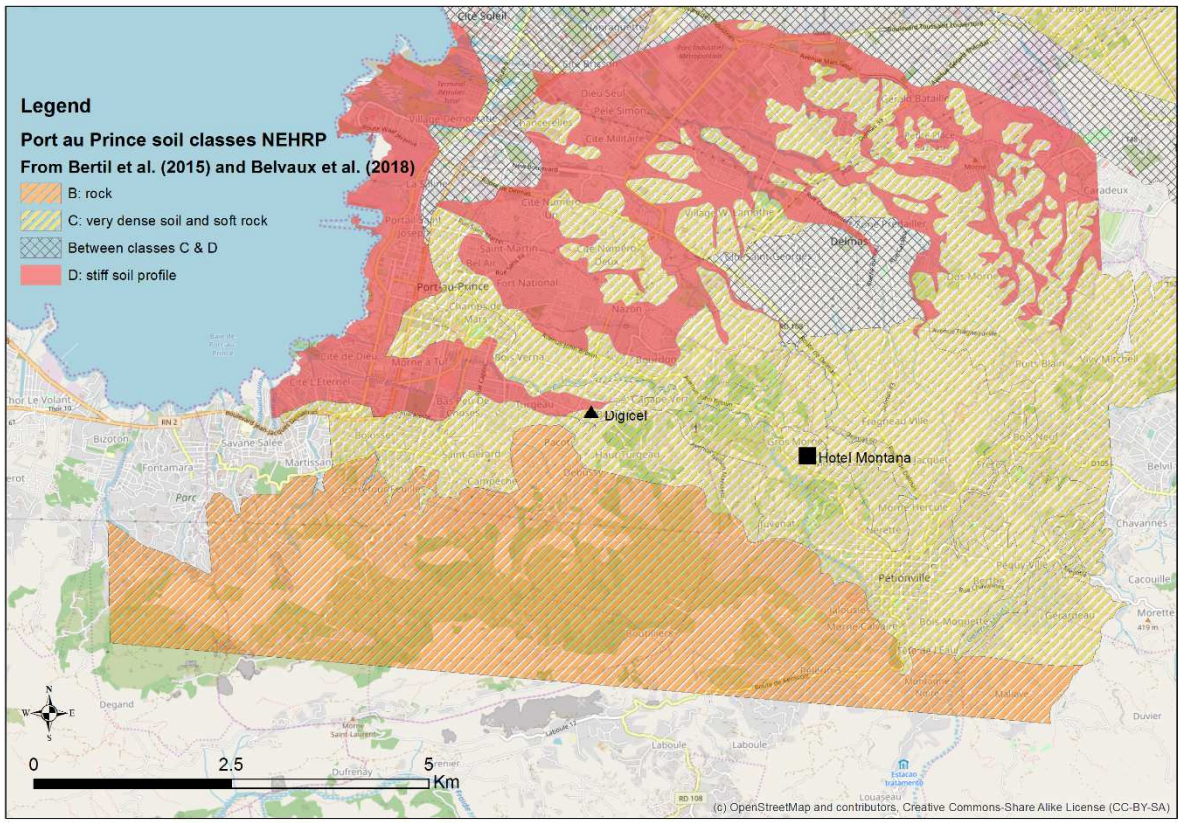

Figure 5: Map of lithological classification for the Port-au-Prince from microzonation (taken from Bertil et al. (2015).

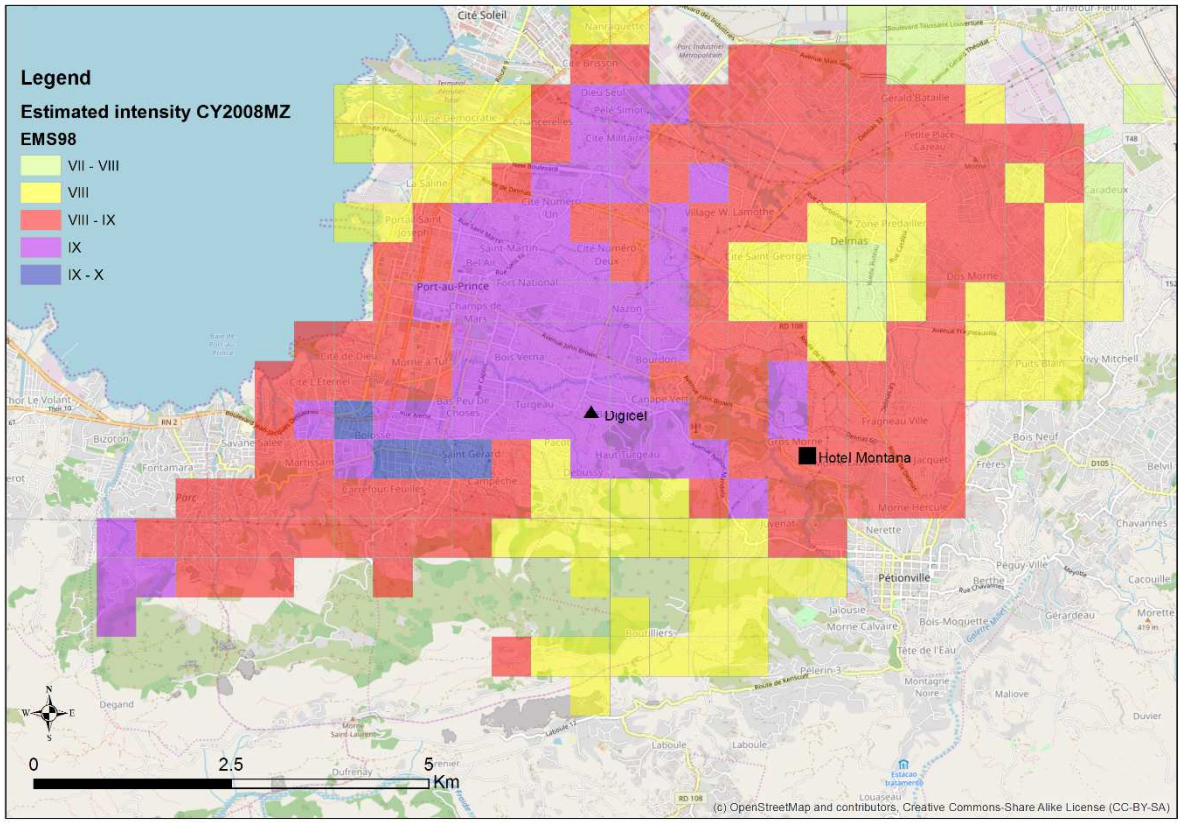

Figure 6: Map of estimated intensity in the Port-au-Prince area using the CY2008 MZ simulation.

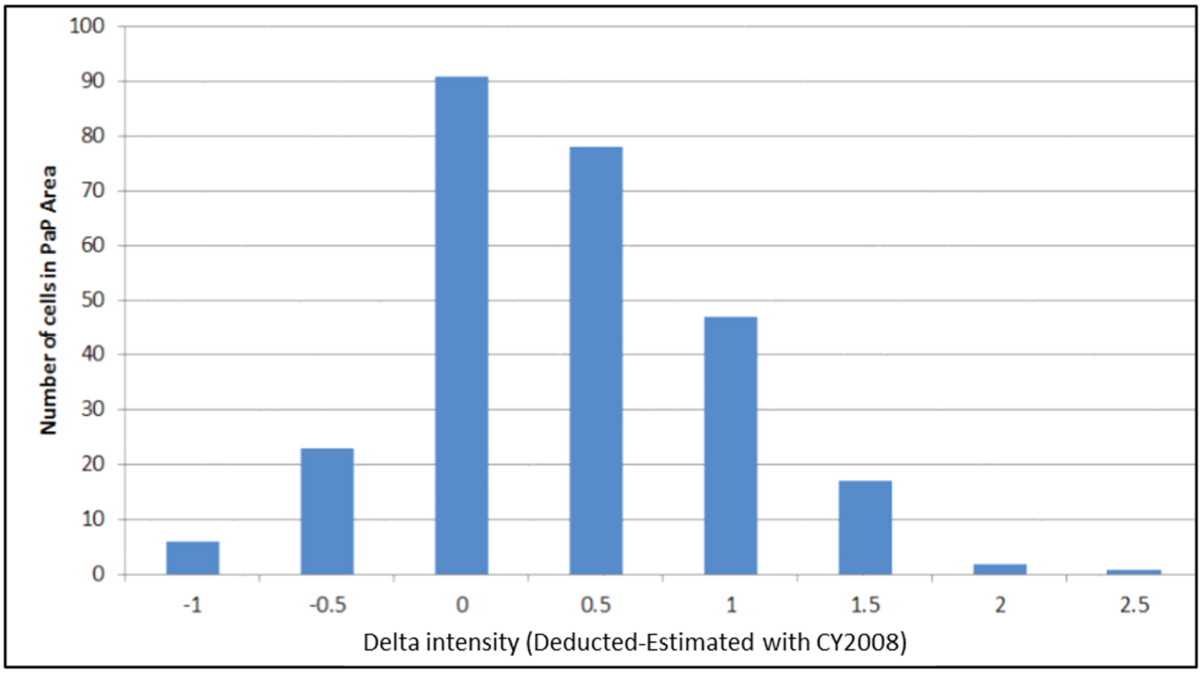

Figure 7: Comparison between our deducted intensity and estimated with CY2008 intensity in the Port-au-Prince area.

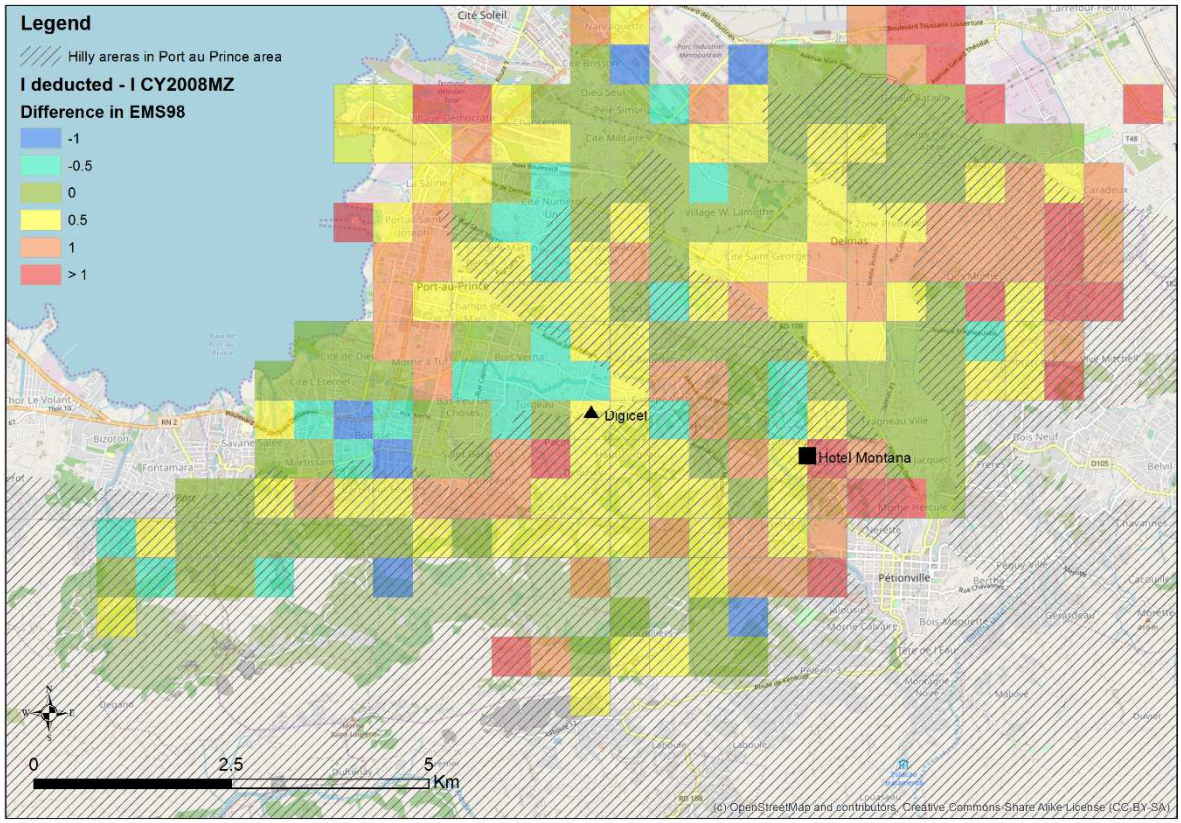

Figure 8: Map of differences (at 0.5 intensity levels) between the deducted intensity and estimated (CY2008MZ) by cell grid of 500 m in the Port-au-Prince area. Green cells correspond to equivalent values; positive values correspond to underestimation using the CY2008 MZ simulation and negative values to overestimation.

We attempted to compare these estimations to instrumental data, but it does not exist in the Port-au-Prince area for the 2010 mainshock. Table 4 compares our estimations to several works that attempted to deduct PGA values in the Port-au-Prince area, based on damage assessment of electrical facilities (Gould et al. 2011) or estimation from horizontal solid rigid movement (Hough, Taniguchi, and Altidor 2012). At Digicel and Hotel Montana our PGA estimations seems to be consistent with their value. However, very high discrepancies appeared when looking at intensities, which may be explained by different interpretations using the MMI or EMS98 scale. In any case, the determination of intensity evaluating damage to individual structures does not seem appropriate.

Looking at the Hotel Montana point in more detail, (Hough et al. 2010) measured a topographical amplification factor varying between 2.3 and 2.5 with an aftershock signal. Taking this value of the topographic amplification factor, we estimated the total amplified PGA at the Hotel Montana site as the following product: PGA of bedrock * lithological amplification factor * topographical amplification factor. Then, we converted it into macroseismic intensity. We estimated a high intensity X, which fits quite well with the observed damage in the area (deducted intensity varies between IX and X). In our work, we did not characterize the topographic factor in the whole area; thus, underestimation was possible in zones with steeper slopes and hills. (Rathje et al. 2011) observes in several districts with shapes with ridges and steep valleys (Hotel Montana, Bois Patate, St Gerard) an over-damage ratio with a collapse ratio varying from 40 to 74%. Recently, (Green 2018) compares building damage dataset with a simulation of PGD amplification due to landslides and topographic factor in Port au Prince area, but he did not find a clear correlation between damages density and PGD. Unsurprisingly damages in fact are a combination of local soil factors (local site effects and landslides), topographic amplification and

local variations in building vulnerability. Moreover, we find "social-economic" correlations like the fact that shanty areas tends to be located in high slope zones.

				Present work		
Point ID	Long/Lat	Deducted PGA (in cm/s²)	Other source intensity	Deducted intensity	Calculated CY2008 PGA (cm/s²)	Calculated CY2008 Intensity
Hotel Montana sector (hill)	-72.297/ 18.527	440[1]	VIII[1]	IX-X	400 (1000 with topographical factor)	VIII-IX (X considering topographical factor)
Digicel (foothill)	-72.3232/ 18.5327	300-470[2,3]	VIII[2]	IX-X	470	IX
HVCV – Canapé Vert (foothill)		300-700[3]	VIII[3]	IX-X	425	VIII-IX
HBME – Delmas (South airport), (flat sector)		150-350[3]	VIII[1],V-VI[3]	VIII-IX	370	VIII-IX
HCEA-Laboule (South Port-au-Prince), reference aftershock station		80-190[3]	VIII[1]	VIII	300	VIII

Table 4: Comparison of deducted PGA and intensity at several points in Port-au-Prince with deducted and calculated PGA and intensity in the present work. Data sources include 1) USGS ShakeMaps (*http://earthquake.usgs.gov/earthquakes/ShakeMap/global/shake/2010rja6/download/stationlist.xml*), 2) Goodno et al. (2011), and 3) Hough et al. (2012).

3.3. Data interpretation - Empirical vulnerability curves

The UWJ dataset has only damaged buildings in areas exposed to higher levels of seismic intensity (>VII-VIII) after the 2010 event. In this work, we attempted to find additional building damage in other earthquakes in the same regional context. The previous largest earthquake on La Hispaniola Island was in 2003, in the north-central part of La Hispaniola near Puerto Plata (Dominican Republic), a Mw 6.5 earthquake, killing 2 persons and injuring 98. USGS Shakemaps estimates its intensity around VI-VII in Puerto Plata city and V-VI in Santiago de los Caballeros city. The Dominican authorities (seismic vulnerability reduction agency, ONESVIE) provided us the location of the heaviest damage and the characteristics of the damaged buildings (8 in D5, 14 in D4, 24 in D3), in addition to the observations in situ from (Lopez Rodriguez and Martinez Cruzado 2003). The total number of buildings in the impacted area, and the total number of undamaged buildings, is unknown; however, the Dominican Stat Data office (ONE) for the 2010 census estimated more than 200,000 dwellings in the impacted area (municipalities near Puerto Plata in addition to Santiago de los Caballeros). Consequently,

we imagined that many buildings were undamaged or had no reported damage (D0-D1), even D2. Heavy damages were not enough significant in number. It is difficult to estimate a damage assessment for this event with this partial dataset.

With UWJ catalog, using the equation 1, we calculate the mean damage grade "μd" for ShakeMap intensity intervals. Equation 2 is used for calculating the standard deviation, which added or subtracted form mean damage grade. The results are shown on Table 5.

$$\mu_D = \sum_{k=0}^{5} p_k * k \qquad 0 < \mu_D < 5 \tag{1}$$

$$\sigma_D = \sqrt{\mu_D \left(1 - \frac{\mu_D}{5}\right)} \tag{2}$$

Once the mean damage grades are calculated using the above equation, we are fitting a set of curves in which beside the intensity and the mean damage grade we are adding the vulnerability index parameter, as presented in equation 3. This equation was developed and used in the framework of FP5 RISK-UE project ((Milutinovic and Trendafiloski 2003) and considers the vulnerability index as follows:

$$\mu_D = 2.5 \left[1 + \tanh\left(\frac{I + 6.25V - 12.8}{2.1}\right)\right] \tag{3}$$

Intensity (ShakeMaps)	UWJ Damage building distribution (in ratio)					μd	σ	μd+σ	μd-σ
	D1	D2	D3	D4	D5				
8	0.55	0.21	0.05	0.07	0.12	2.01	1.10	3.11	0.92
8.5	0.73	0.00	0.05	0.11	0.11	1.88	1.08	2.97	0.80
9	0.71	0.12	0.05	0.06	0.06	1.65	1.05	2.70	0.60
9.5	0.49	0.26	0.10	0.07	0.08	2.00	1.10	3.10	0.91

Table 5: Field investigation data coming from UWJ catalog combined with ShakeMap intensity values for January 12, 2010 Haiti earthquake. Calculation of mean damage grades and standard deviation.

The fragility curves based on 4 values of vulnerability index following the RISK-UE methodology are compared with mean damage from 2010's (Table 5) and 2003's earthquakes in Figure 9. Surprisingly mean damage μd do not increases when ShakeMap intensity increases. As discussed in the previous sections, this can be due to accuracy of ShakeMap intensity at this scale of work. It seems that there is no a clear spatial correlation between damages and intensity from ShakeMap.

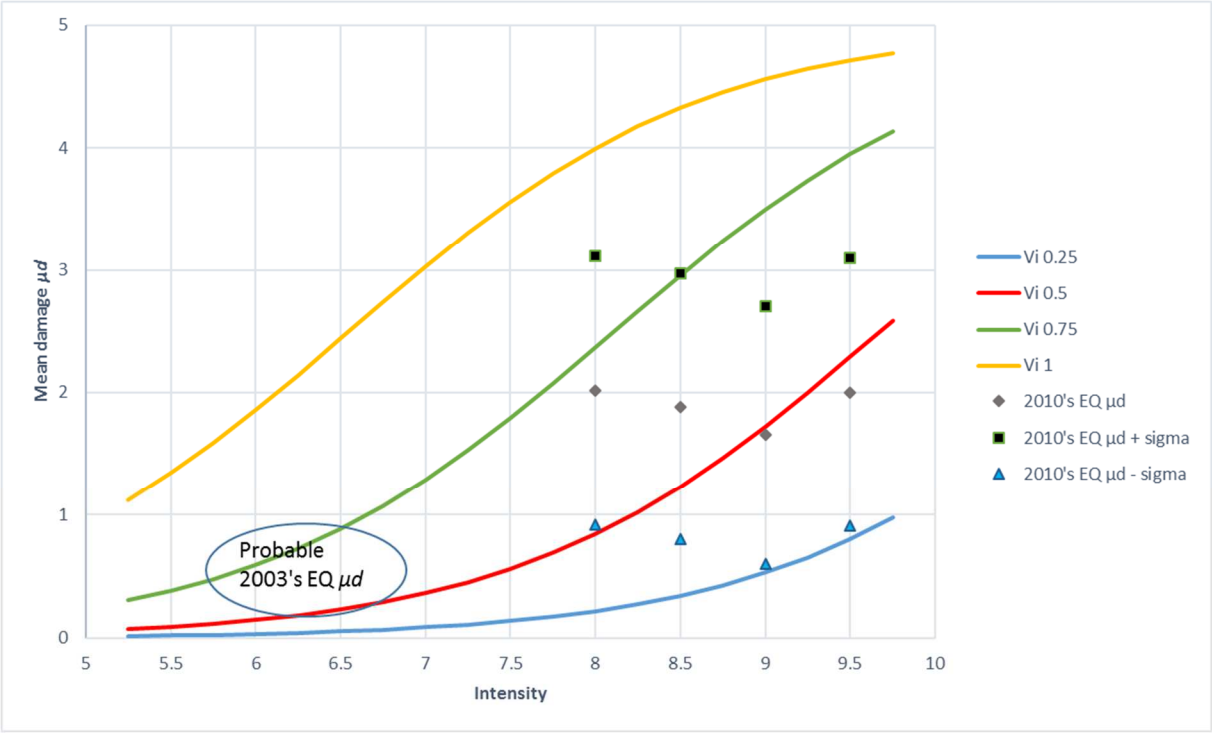

Figure 9: fragility curves based on RISK-UE indexes and mean damage for 2010's Earthquake. The probable, but not calculated, mean damage for 2003's earthquake is shown.

Discrepancies can also come from UWJ catalog. UWJ dataset were obtained using remote sensing techniques and present an inventory of a large number of buildings (299,257) which is, generally, very useful for statistical analysis. The downside of these types of methods is that the detection of the damage degree is difficult. Indeed, the damage degree that represents large deformation of the structure is well identified (D4 and D5), but the intermediary damage degrees that represent small deformation structural damage (D3) and/or non-structural damage (D1 and D2) are quite difficult to observe. For the intensity equal or exceeding VII-VIII more than 60% of buildings showed no visual damage D1 (Table 5). This value surely cannot represent the reality.

(Ufuk Hancilar, Taucer, and Corbane 2013) works with the UWJ dataset and combines it with ShakeMap intensity in order to produce vulnerability functions. The first family of curves were given by built areas density (Figure 10). As it can be seen, they had to manage with a catalog poor damage data in low-moderate intensities (<=VII). If this task of the completeness of the data for the small intensity values is not performed, the fragility curves obtained show poor results, as for example only 5% damaged structures (D3) for an intensity equal to VIII (Figure 10). In this case, for construction of reliable fragility curves, the observational data should be numerically completed, for the lower intensity values.

The remote sensing observational data of damages after an earthquake do not discriminate the structural type, but they are considering the level of density of considered area (e.g. Low-density built-up zone, Medium-density built-up zone …). Therefore, in order to have information about the structural type, the huge amount of remote sensing data has to be coupled with others type of data, like field observations. (Ufuk Hancilar, Taucer, and Corbane 2013) have done an important work in which the main purpose of the targeted field campaign was to validate the remote sensing based damage assessment. Using the parameters (median and

lognormal standard deviation) from the study of (Ufuk Hancilar, Taucer, and Corbane 2013), Figure 10 presents the comparative fragility curves derived by the sub-sets of remote sensing for low-density build-up zone and for high-density build-up zone. Only the damages degrees D3, D4 and D5 were considered and the aggregation of D2 and D1, as well as no damage (D0), into one category was considered, since that for these classes, there is no visible damage in remote sensing based assessment. As observed in the Figure 10, the ground motion intensities for buildings in the remote sensing dataset range between 7.4–9.8

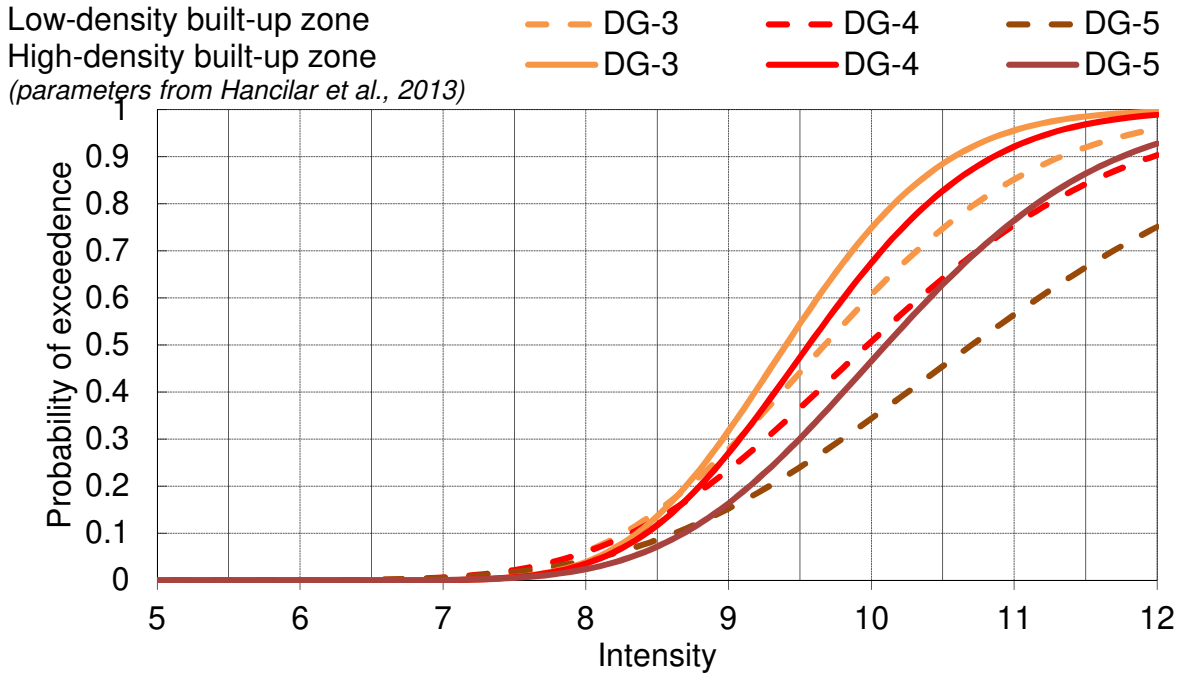

Figure 10: Fragility curves based on remote sensing observations for high-density and low-density built-up zone (median and standard deviation parameters form Hancilar et al., 2013)

For a damage scenario, we need to complete these range of intensities with the intensities inferior to 7.4. In the next step, we are trying to calibrate these curves to the manner of description of the fragility curves proposed by the RISK-UE methodology. To take advantage of the remote sensing observations for the extensive damage degrees and to improve or calibrate them for a lower damage degree we plotted these data and literature-equivalent data against intensity value (Figure 11 to Figure 14).

Figure 11 shows the curves based on the Haiti observed data (dashed lines) for high-density built-up zone and the curves calculated based on the RISK-UE methodology for a vulnerability index of Vi=0.522, which corresponded to the most vulnerable Concrete Moment Frame typology. Figure 12 uses a vulnerability index of Vi=0.672 considering the previous value and a supplementary vulnerability factor because of the pre- or low-code construction period (+0.16) as described in the RISK-UE methodology.

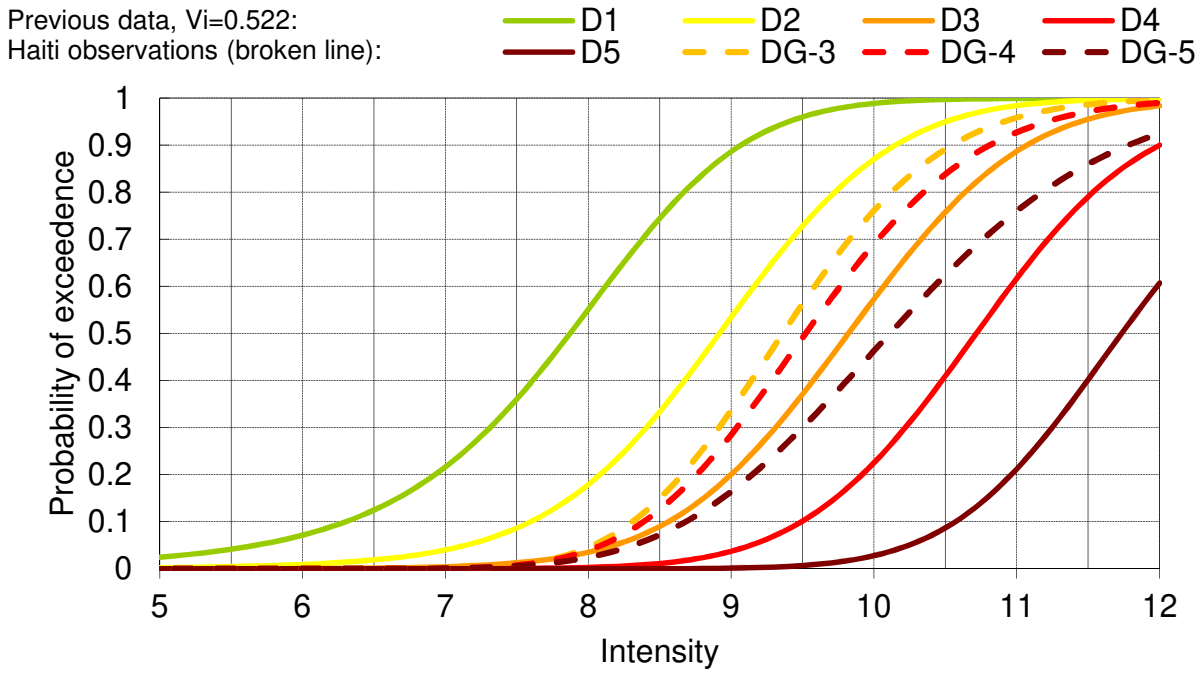

Figure 11: Fragility curves based on damage observations and comparison to the RISK-UE (Vi=0.522).

It is apparent that the difference between the D4 and D5 curves is not as important, particularly for Vi=0.672. This seems realistic because it can be considered without much error, that the same typology of structure is more vulnerable in Haiti than in Europe from a construction practice point of view. Therefore, the higher probability of having D4 and D5 using the remote sensing data is useful to adapt the fragility curves to regional construction.

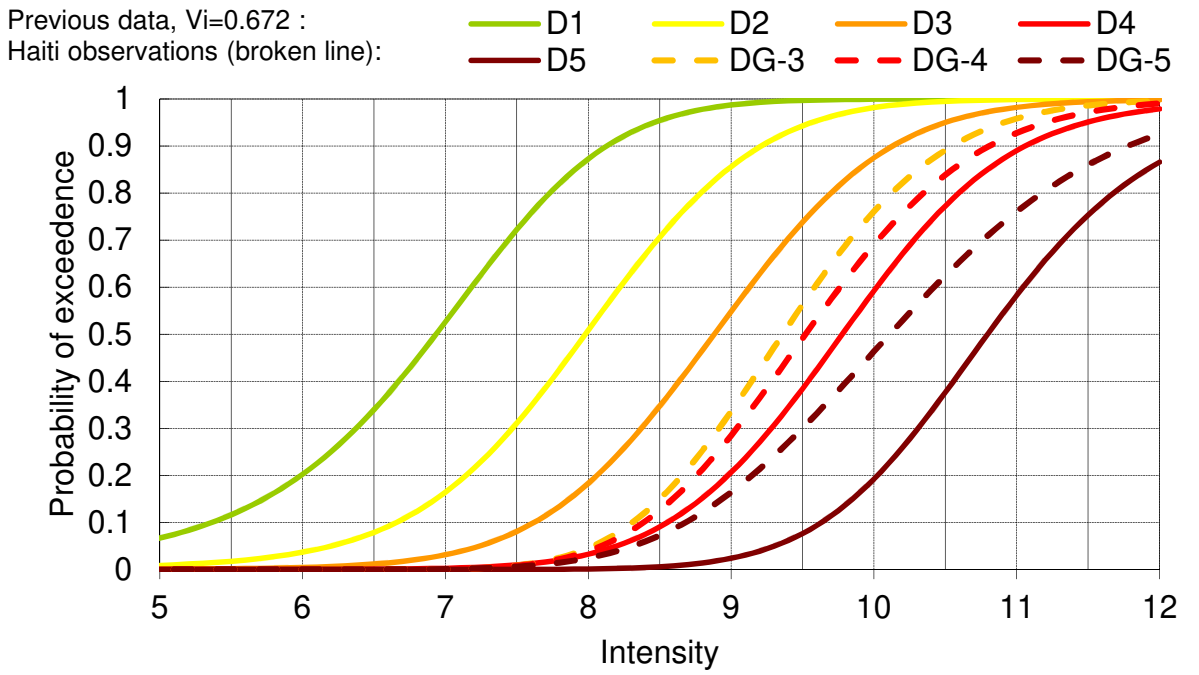

Figure 12: Fragility curves based on damage observations and comparison to the RISK-UE (Vi=0.672).

Figure 13 and Figure 14 show the coefficient that can be used if we want to "calibrate" the existing empirical fragility curves to those obtained using the remote sensing observation after the earthquake event. This "shift/calibration" is necessary for areas in which the regional context for building is unknown, and hence we are obliged to adapt exiting curves derived from other regional areas, but also for the data coming only from the remote sensing services. (Ufuk Hancilar, Taucer, and Corbane 2013) said that the omission errors (e.g. number of buildings omitted from a damage state by remote sensing assessment as a percentage of the total number of buildings assigned to that damage state by field observations) for damage grades DG-0-1-2, DG-3, DG-4, and DG-5 were 26%, 94%, 70%, and 53%, respectively. This suggests that there is high discrepancy between field and remote sensing data, particularly for DG-3 and DG-4, and even for DG-5. Hence, Figure 13 propose a “calibration factor” relative to the damage degree D3 and Figure 14 relative to the damage degree D4. In order to calculate the value of the “calibration factor”, we try to superpose the respective fragility curve (D3 or D4) coming from the remote sensing with the one coming from the RISK-UE methodology, by considering that the 50% of probability of exceedance is the same for both curve (red round in Figure 13 and 14). That “calibration factor” shifts all the set of the fragility curves to the right or to the left, which mean that only the fragility curves of the targeted damage degree (D3 or D4) will be superposed, and the other fragility curves will cover all the range of the intensities.

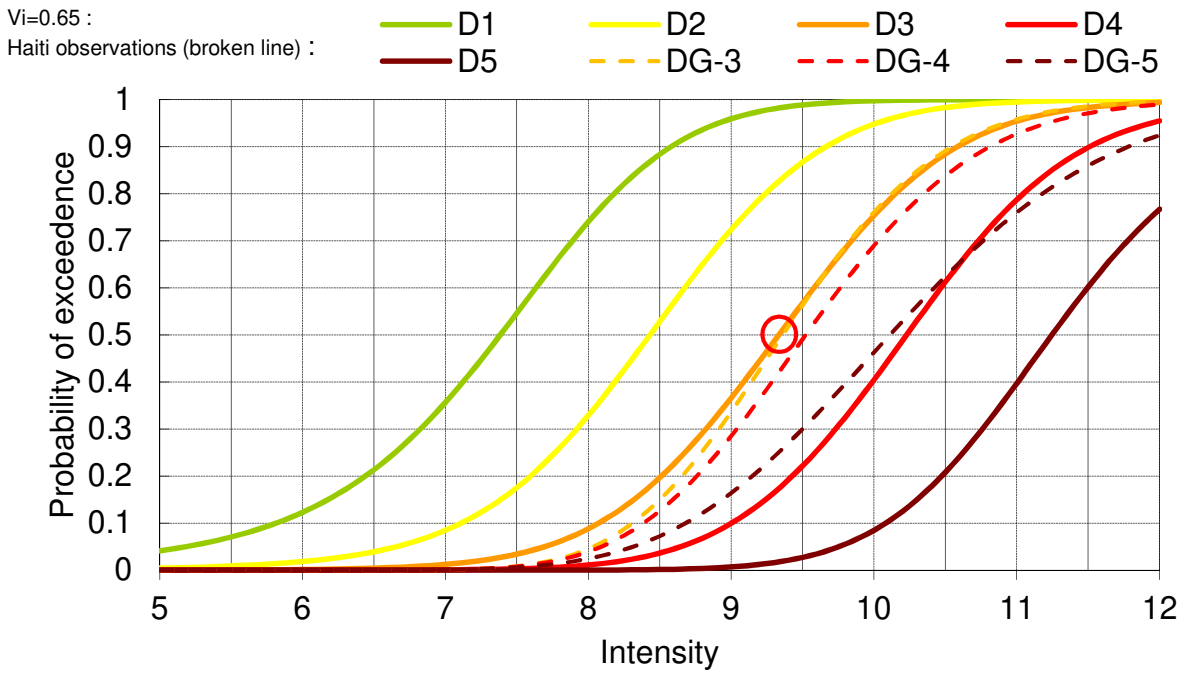

Figure 12: Fragility curves based on remote sensing observations and comparison to the RISK-UE fragility curves (vulnerability index Vi=0.522 and correction factor of 0.128) for calibration of the median value of the D3 damage degree.

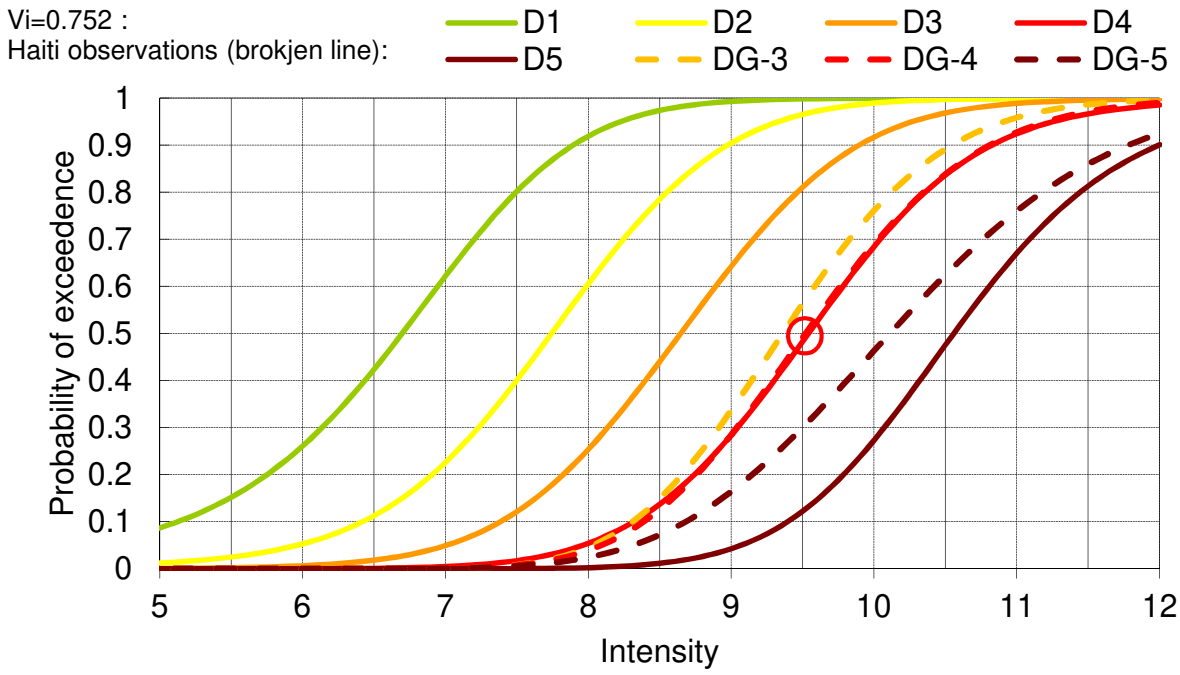

Figure 13: Fragility curves based on remote sensing observations and comparison to the RISK-UE (vulnerability index Vi=0.522 and correction factor of 0.23) for calibration on the median value of the D4 damage degree.

4. Damage scenario

Several post-earthquake damage scenarios have been completed using the Armagedom software (Sedan et al. 2013). This software computes damage using the RISK-UE methodology of level 1 (Milutinovic and Trendafiloski 2003; Lagomarsino and Giovinazzi 2006) and vulnerability indexes and macroseismic intensity as input.

We only calculated post-earthquake damage scenarios for the Port-au-Prince municipality. The distribution of buildings types in the 36 districts in Port-au-Prince was provided by (Benito et al. 2012) (Figure 15). They distinguished all residential buildings of six building types, which were associated with the building types from (Lagomarsino and Giovinazzi 2006) termed L&G. The most frequent building type was RCCB, which has reinforced concrete frames with masonry infill walls. Nearly 60% of the buildings in each district were in this category. The most important differences in terms of building types among the districts appears in the presence or absence of reinforced concrete shear-walls (RCSW), unreinforced masonry (URM), and confined masonry (RLBM).

Some authors have worked on capacity curves and fit them to Haitian building stock (Molina et al. 2014; Torres et al. 2016); in the present work, addressing deducted or observed intensities, we proposed to calculate damage scenarios based on vulnerability indexes.

Based on the aforementioned relation between the Haitian building types and L&G types, we proposed to use two sets of L&G vulnerability indexes. The first set considers vulnerability indexes from L&G and adds +0.08 as an aggravation factor for no seismic code cases. The second set adds +0.16, as a "regional correction." These correction values are those proposed usually when using RISK-UE

methodology to assess current building vulnerability ((Lagomarsino and Giovinazzi 2006; Milutinovic and Trendafiloski 2003)

As previously shown in Figures 11 to 13 vulnerability indexes between 0.6 and 0.75 fit quite well with empirical functions if looking only at very heavy damage (D4) and to the intermediate damage degree if a shift-correction factor to the D3 damage degree is applied.

Table 7 presents the six scenarios' main characteristics. Two parameters change, the two sets of vulnerability indexes and three seismic intensity maps: the USGS ShakeMap, intensity CY2008, and deducted intensity map obtained using the interpretation of damage of the UWJ dataset. The flowchart in the Figure 16 shows the relation between the different datasets and data sources used, calculated or estimated in the present work.

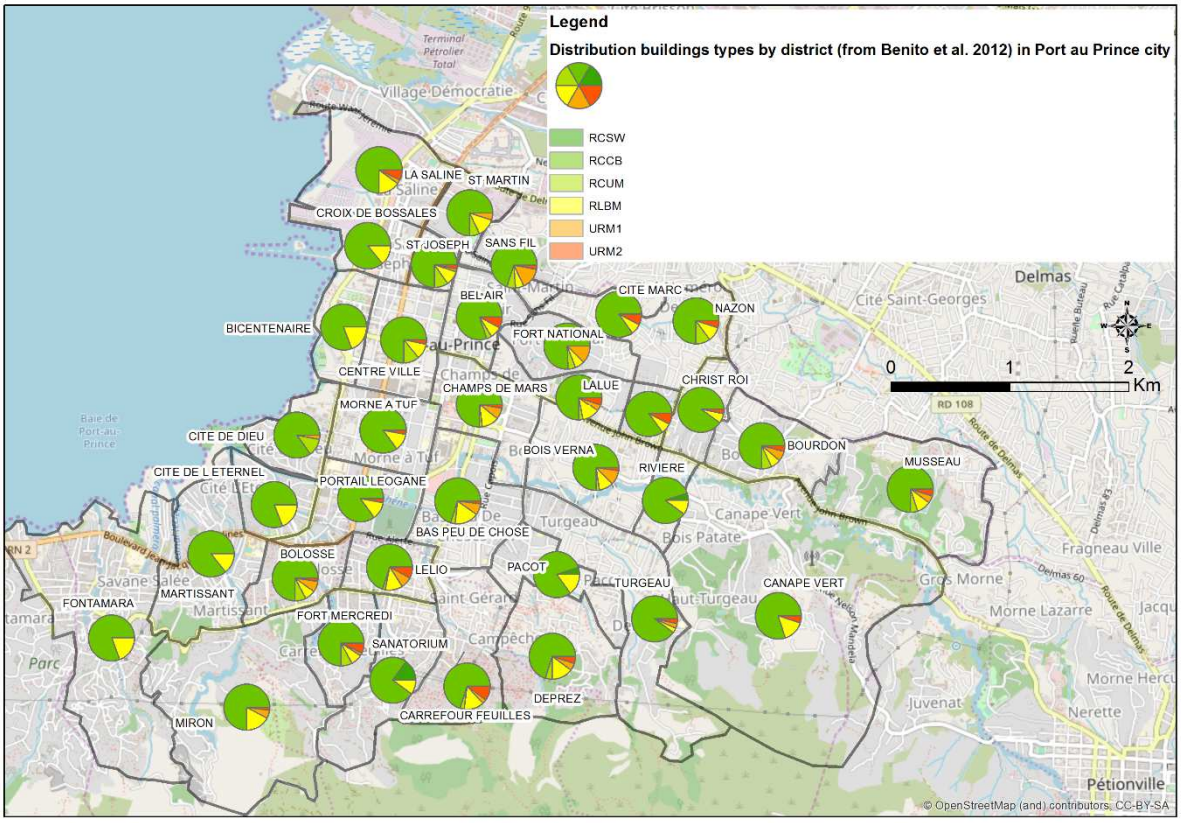

Figure 15: Distribution of building types by district in the Port-au-Prince municipality. Taken from Benito et al. (2012).

Building type (Torres et al. 2016)	Type L&G	Description	Vi L&G + 0.08 (no code)	Vi L&G + 0.08 (no code) + 0.08 (regional correction)

RCSW	RC2-1	Reinforced concrete shear walls, without code and poor maintenance	0.62	0.7
RCCB	RC1-1	Reinforced concrete frames – masonry infill walls, without code and poor maintenance	0.72	0.8
RCUM	RC1-1	Reinforced concrete frames – masonry infill walls, without code and poor maintenance	0.72	0.8
RLBM	M7 precode	Confined/reinforced masonry, poor maintenance, poor connection roof/walls	0.53	0.61
URM1	M6 precode	Unreinforced masonry concrete slabs, poor maintenance, poor connection roof/walls	0.696	0.776
URM2	M5 precode	Unreinforced masonry – wooden frames, poor maintenance, poor connection roof/walls	0.82	0.9

498 Table 6: RISK-UE vulnerability indexes for the main building types in Port-au-Prince.

499

Scenario	Seismic intensity input	Vulnerability distribution
SC1	CY2008	Benito et al. 2012 building types distribution
SC2	USGS ShakeMap	
SC3	Local intensity deducted from JRC catalog	Lagomarsino and Giovinazzi (2006) Vi + aggravant factor 0.08
SC4	CY2008	Benito et al. 2012 building types distribution
SC5	USGS ShakeMap	
SC6	Local intensity deducted from JRC catalog	Lagomarsino and Giovinazzi (2006) Vi + aggravant factor 0.16

500 Table 7 : Main characteristics of damage scenarios in terms of seismic intensity input and vulnerability
501 distribution.

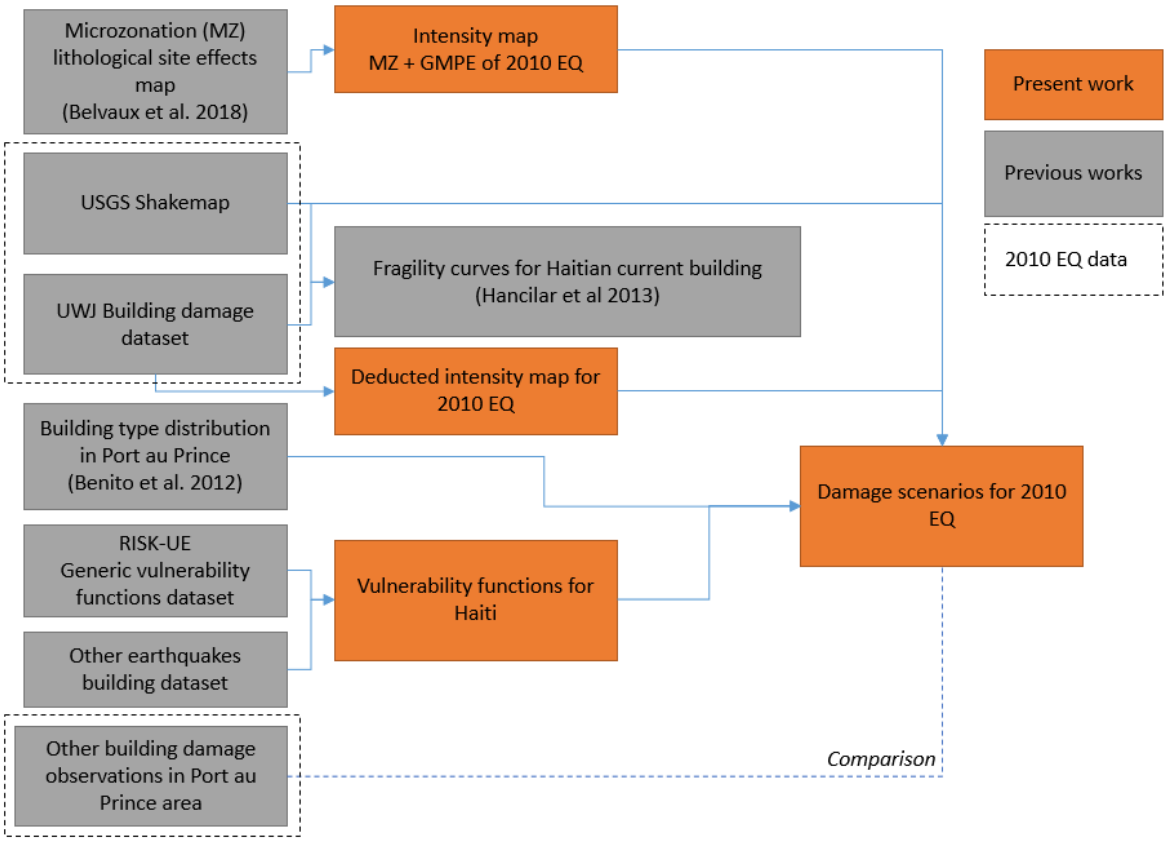

Figure 16: flowchart showing the relation between the different data sources used in the present work.

5. Discussion

Table 8 show the results of the six damage scenarios, in terms of % and number of buildings in the D3, D4 and D5 damage states, in addition to the values of the UWJ dataset in the Port-au-Prince municipality. Results show the great influence of vulnerability functions and confirms that the global building stock in Port-au-Prince was very vulnerable. The damage scenarios' estimated number of buildings in the D3 damage state is very high when compared to that of the UWJ dataset. Moderate damage states are difficult to evaluate using only aerial images. Some authors (Saito et al. 2010), with a very limited field survey dataset, have estimated that heavy damage reached 46% in Port-au-Prince, whereas the Pictometry or aerial image estimates between 20 and 30%. We can interpret this as many buildings tagged as D3 in the UWJ dataset are in reality D4 or D5. More pessimistic vulnerability values (SC4 to SC6) gives strong damage ratios, only comparable with (Saito et al. 2010) observations. Results from SC1 to SC3 vulnerability values corresponds quite well with other observations datasets (GEO-CAN, Pictometry, MTPTC). Maybe these values are those the most appropriated for Haiti building stock.

Results obtained using the initial ShakeMaps (SC2 and SC5) underestimated heavy damage because ShakeMaps estimates mainly an intensity VIII in Port-au-Prince, which is, in our opinion, an underestimation of the intensity by one level as discussed previously. Increasing the intensity respect ShakeMaps, the important damages (the sum of D3, D4 and D5) are greater, differing heavily with UWJ dataset. We cannot reproduce the low value of buildings in D3. This kind of situation could correspond to a situation with two families of buildings in Port au Prince, very vulnerable and very low vulnerable, but field reports did not notice the existence of an important group of low vulnerable buildings, so we do not consider this option.

Scenario	% D3	% D4	% D5	ND3	ND4	ND5
SC1	29.4%	17.8%	3.6%	27516	16610	3349
SC2	27.5%	12.0%	1.3%	25718	11166	1238
SC3	30.0%	22.4%	6.4%	28001	20895	5947
SC4	30.9%	27.3%	9.4%	28901	25531	8808
SC5	32.8%	22.2%	4.4%	30656	20719	4153
SC6	28.9%	30.4%	14.6%	27001	28431	13685
Observed UWJ (buildings tagged "Port-au-Prince" municipality in dataset)	5.6%	11.67%	12.58%	5230	10801	11633
GEO-CAN		23.5%				
MTPTC		16-21%				
EEFIT		46%				
Pictometry		19-28%				

Table 8: Results of post-earthquake damage scenarios.

6. Conclusions

The seismic intensity is extremely important when constructing empirical fragility functions for buildings. In the Port-au-Prince earthquake, instrumental data was so poor or nonexistent that seismic intensity considered in empirical damage functions was mostly from simulations and models. For earthquakes in developing countries with a very low density of seismological stations, tools such as USGS ShakeMaps are of great importance in the minutes, hours, and days after the earthquake. However, in these cases, ShakeMaps is not the definitive version of "what happened," because it heavily depends on first parameter estimation. It is also important to consider the representativeness of less damaged areas and complete the building damage dataset in these areas (intensities VI or VII, for example). If nothing else, empirical damage functions could appear too "vertical," passing very quickly from no-damage to strong-damage.

Exhaustive building damage datasets are a tool and set of data suitable for many applications. In the case of Haiti, several datasets exist, collected by a multitude of actors and organizations that collaborated to build them. Even though the damage datasets such as UWJ are incomplete, they are still the most exhaustive, but do not describe the reality, mostly in terms of moderate state damage, which is very difficult or impossible to identity using aerial/satellite imagery. Even with field survey controls, many authors have highlighted this risk of underestimation. However, this dataset remains a reference.

A huge building damage database permits one to map damage and consequently macroseismic intensity at a very small scale (in our work 500-m cells) based on EMS98 damage-intensity conversion criteria. The basis of this work was to consider the intensity statistically representative of an area, and not based on only punctual observations. This intensity map, called "deducted intensity," corresponds quite well with the perceived intensity (MMI=IX (Cambridge Architectural Research Ltd 2010)). In any case, in the Port-au-Prince area, one can see strong damage variations, which induces strong intensity differences. In our opinion, global building vulnerability is quite constant (without strong spatial disparities) and consequently intensity variation should be to the result of other factors: lithological or topographical site effects, landslides, and attenuation of ground motion at a Port-au-Prince scale. Based on the seismic microzonation completed in Port-au-Prince (Bertil et al. 2015; Belvaux et al. 2018) we

attempted to match the deducted intensity map with a classical approach to estimate intensity (calculation of PGA by GMPE, consideration of microzonation and lithological amplification, and conversion in intensity). In a large number of cells, the estimated intensity fits the deducted. In another important number of cells, the deducted intensity is higher than that estimated (perhaps because of topographic effects).

Finally, we calculated seismic damage scenarios for the Port-au-Prince municipality using the RISK-UE method of vulnerability indexes, adapting the indexes to the Haitian context and previous works in terms of vulnerability assessment of the current Haitian buildings. First, the results of the damage scenarios show the great influence of vulnerability functions and confirms that the global building stock in Port-au-Prince was very vulnerable. Second, intensity maps also have a strong influence; during the first hours ShakeMap, for example, underestimated the damage. Post-earthquake investigations obtain elements to understand the high damage level in Port-au-Prince. In addition, damage scenarios cannot reproduce the situation of many buildings with heavy damage (D4 and D5), only a few buildings with moderate damage (D3), and many buildings with minor/no damage. Is the building damage dataset exhaustive for moderate damage? We do not believe so. Even if the damage scenarios are not at all the damage reality, some damage scenario results are nearer to those of several observers, aerial/satellite datasets that still underestimate moderate/heavy damage. Remote sensing images combined with aerial or semi aerial images (such as Pictometry) are a precious tool for the first trends of damage and in prior damaged areas, but field survey control is necessary for moderately damaged buildings. In the case of Haiti, but probably in many other cases, it would be better to combine in the same dataset the UWJ data (mostly from satellite-aerial assessment) with the habitability assessment from the MTPC dataset.

Acknowledgements

Various programs of seismic microzonation for vulnerable cities of Hispaniola Island cited in this paper were conducted by the BRGM in partnership with Laboratoire National du Bâtiment et des Travaux Publics (LNBTP) and Bureau des Mines et de l'Energie in Haiti, and with Servicio Geológico Nacional (SGN) and Instituto Geológico y Minero de España (IGME) in the Dominican Republic. These studies were part of the United Nations Development Programs "The seismic risk reduction plan for northern Haiti (2012–2016)" and the "Estudio de la amenaza sísmica y vulnerabilidad física del Gran Santo Domingo (2013–2016)." We thank the anonymous reviewers for their careful reading of our manuscript and their many insightful comments and suggestions.

References

Atkinson, Gail M, and Eleanor Sonley. 2000. "Empirical Relationships between Modified Mercalli Intensity and Response Spectra." *Bulletin of the Seismological Society of America* 90 (2): 537–44. http://dx.doi.org/10.1785/0119990118.

Belvaux, Myriam, Kristel Meza-Fajardo, Jaime Abad, Didier Bertil, Agathe Roullé, Santiago Muñoz, and Claude Prépetit. 2018. "Combined Geophysical and Geotechnical Approaches for Microzonation Studies in Hispaniola Island." *Geosciences* 8 (9).

Benito, B., J. Cervera, J. Gaspar, A. Staller, S. Martinez, A. Rivas, Y. Torres, et al. 2012. "Projet Sismo-Haïti. Evaluation de l'aléa et Su Risque Sismique En Haïti Dirigée Vers La Conception Parasismique."

Bertil, D., Claude Prépetit, A. Roullé, Jean-Philippe Rançon, and A. Vagner. 2015. "Seismic Microzonation in Haiti: An Important Tool for Seismic Risk Mitigation." UNISDR. https://www.preventionweb.net/files/workspace/7935_vagneretalhaitian.pdf.

BSSC. 2003. *NEHRP RECOMMENDED PROVISIONS FOR SEISMIC REGULATIONS FOR NEW*

BUILDINGS AND OTHER STRUCTURES (FEMA 450). Part 1: Provisions. 2003rd ed. FEMA.

Calais, Eric, Andrew Freed, Glen Mattioli, Falk Amelung, Sigurjón Jónsson, Pamela Jansma, Sang-Hoon Hong, Timothy Dixon, Claude Prépetit, and Roberte Momplaisir. 2010. "Transpressional Rupture of an Unmapped Fault during the 2010 Haiti Earthquake." *Nature Geoscience* 3 (October): 794. http://dx.doi.org/10.1038/ngeo992.

Cambridge Architectural Research Ltd. 2010. "Port-Au-Prince Earthquake Damage Assessment Using Pictometry" 44 (June).

Chiou, BrianS-J., and Robert R Youngs. 2008. "An NGA Model for the Average Horizontal Component of Peak Ground Motion and Response Spectra." *Earthquake Spectra* 24 (1): 173–215. https://doi.org/10.1193/1.2894832.

Conseil de l'Europe. 1998. *Cahiers Du Centre Européen de Géodynamique et de Séismologie. European Macroseismic Scale 1998*. Vol. 15.

Cooner, Austin J, Yang Shao, and James B Campbell. 2016. "Detection of Urban Damage Using Remote Sensing and Machine Learning Algorithms: Revisiting the 2010 Haiti Earthquake." *Remote Sensing* 8 (10).

Copernicus. 2015. "How the Copernicus Emergency Management Service Supported Crisis Preparedness and Response Operations in Nepal." Copernicus Newsletter. 2015. http://newsletter.copernicus.eu/issue-12-december-2015/article/how-copernicus-emergency-management-service-supported-crisis.

Copernicus EMS. 2016. "EMSR159: Earthquake in Ecuador." 2016. http://emergency.copernicus.eu/mapping/list-of-components/EMSR159.

Corbane, Christina, Keiko Saito, Luca Dell Oro, Einar Bjorgo, Stuart P D Gill, Boby Emmanuel Piard, Charles K Huyck, et al. 2010. "A Comprehensive Analysis of Building Damage in the 12 January 2010 M w 7 Haiti Earthquake Using High-Resolution Satellite- and Aerial Imagery," no. January.

Dong, Laigen, and Jie Shan. 2013. "A Comprehensive Review of Earthquake-Induced Building Damage Detection with Remote Sensing Techniques." *ISPRS Journal of Photogrammetry and Remote Sensing* 84: 85–99. https://doi.org/https://doi.org/10.1016/j.isprsjprs.2013.06.011.

Douglas, J., D. Monfort, C. Negulescu, A. Roullé, and O. Sedan. 2015. "Limits on the Potential Accuracy of Earthquake Risk Evaluations Using the L'aquila (Italy) Earthquake as an Example." *Annals of Geophysics* 58 (2). https://doi.org/10.4401/ag-6651.

EagleView. n.d. "Pictometry Imagery." https://www.eagleview.com/product/pictometry-imagery/#.

Ehrlich, Daniele, Michele Melchiorri, Aneta J Florczyk, Martino Pesaresi, Thomas Kemper, Christina Corbane, Sergio Freire, Marcello Schiavina, and Alice Siragusa. 2018. "Remote Sensing Derived Built-Up Area and Population Density to Quantify Global Exposure to Five Natural Hazards over Time." *Remote Sensing* 10 (9). https://doi.org/10.3390/rs10091378.

Ghosh, Shubharoop, Charles K Huyck, Marjorie Greene, Stuart P Gill, John Bevington, Walter Svekla, Reginald Desroches, and Ronald T Eguchi. 2011. "Crowdsourcing for Rapid Damage Assessment : The Global Earth Observation Catastrophe Assessment Network (GEO-CAN)" 27 (October): 179–98. https://doi.org/10.1193/1.3636416.

Giovinazzi, Sonia. 2005. "The Vulnerability Assessment and the Damage Scenario in Seismic Risk Analysis," no. May 2005: 222.

Gould, P L, B J Goodno, N C Gould, and P Caldwell. 2011. "Behavior of Engineer Constructed Facilities in the Haitian Earthquake of January 12 , 2010." *Procedia Engineering* 14: 23–31. https://doi.org/10.1016/j.proeng.2011.07.003.

Green, Rupert. 2018. “The Effects of Topography on Seismic Motion of the 2010 Mw 7.0 Haiti Earthquake and Associated Damages.” University of Twente. https://library.itc.utwente.nl/papers_2018/msc/aes/green.pdf.

Hancilar, U, F Taucer, and C Corbane. 2010. “Empirical Fragility Assessment after the January 12 , 2010 Haiti Earthquake” 44: 353–65. https://doi.org/10.2495/RISK120301.

Hancilar, Ufuk, Fabio Taucer, and Christina Corbane. 2013. “Empirical Fragility Functions Based on Remote Sensing and Field Data after the 12 January 2010 Haiti Earthquake” 29 (4): 1275–1310. https://doi.org/10.1193/121711EQS308M.

Hough, Susan E., Jean Robert Altidor, Dieuseul Anglade, Doug Given, M. Guillard Janvier, J. Zebulon Maharrey, Mark Meremonte, B. S L Mildor, Claude Prepetit, and Alan Yong. 2010. “Localized Damage Caused by Topographic Amplification during the 2010 M7.0 Haiti Earthquake.” *Nature Geoscience* 3 (11): 778–82. https://doi.org/10.1038/ngeo988.

Hough, Susan E, Tomoyo Taniguchi, and Jean-robert Altidor. 2012. “Estimation of Peak Ground Acceleration from Horizontal Rigid Body Displacement : A Case Study in Port-Au-Prince , Haiti” 102 (6): 2704–13. https://doi.org/10.1785/0120120047.

Karimzadeh, Sadra, and Masashi Mastuoka. 2017. “Building Damage Assessment Using Multisensor Dual-Polarized Synthetic Aperture Radar Data for the 2016 M 6.2 Amatrice Earthquake, Italy.” *Remote Sensing* 9 (4).

Lagomarsino, Sergio, and Sonia Giovinazzi. 2006. “Macroseismic and Mechanical Models for the Vulnerability and Damage Assessment of Current Buildings.” *Bulletin of Earthquake Engineering* 4 (4): 415–43. https://doi.org/10.1007/s10518-006-9024-z.

Lemoine, G, and C Corbane. 2013. “Intercomparison and Validation of Building Damage Assessments Based on Earthquake Imagery Using Multi-Source Reference Data,” 1445–86. https://doi.org/10.5194/nhessd-1-1445-2013.

Lopez Rodriguez, R, and J. A. Martinez Cruzado. 2003. “DAÑOS OBSERVADOS EN PUERTO PLATA, REPÚBLICA DOMINICANA, CAUSADOS POR EL TERREMOTO DEL 22 DE SEPTIEMBRE DE 2003.” *Rev. Int. de Desastres Naturales, Accidentes e Infraestructura Civil* 3 (2): 189–204. https://www.scipedia.com/public/Rodríguez_Cruzado_2003a.

Milutinovic, Z., and S. Trendafiloski. 2003. “WP4 Vulnerability of Current Buildings.”

Miyamoto, H Kit, M Eeri, Amir S J Gilani, and Ken Wong. 2011. “Massive Damage Assessment Program and Repair and Reconstruction Strategy in the Aftermath of the 2010 Haiti Earthquake” 27 (January 2010): 219–37. https://doi.org/10.1193/1.3631293.

Molina, S., Y. Torres, B. Benito, M. Navarro, and D. Belizaire. 2014. “Using the Damage from 2010 Haiti Earthquake for Calibrating Vulnerability Models of Typical Structures in Port-Au-Prince (Haiti).” *Bulletin of Earthquake Engineering* 12 (4): 1459–78. https://doi.org/10.1007/s10518-013-9563-z.

Musson, Roger M W, Gottfried Grünthal, and Max Stucchi. 2010. “The Comparison of Macroseismic Intensity Scales.” *Journal of Seismology* 14 (2): 413–28. https://doi.org/10.1007/s10950-009-9172-0.

Piscini, Alessandro, Vito Romaniello, Christian Bignami, and Salvatore Stramondo. 2017. “A New Damage Assessment Method by Means of Neural Network and Multi-Sensor Satellite Data.” *Applied Sciences* 7 (8): 781. https://doi.org/10.3390/app7080781.

Rathje, Ellen M., Jeff Bachhuber, Ranon Dulberg, Brady R. Cox, Albert Kottke, Clinton Wood, Russell A. Green, Scott Olson, Donald Wells, and Glenn Rix. 2011. “Damage Patterns in Port-Au-Prince during the 2010 Haiti Earthquake.” *Earthquake Spectra* 27 (SUPPL. 1). https://doi.org/10.1193/1.3637056.

694 Romaniello, Vito, Alessandro Piscini, Christian Bignami, Roberta Anniballe, and Salvatore
695 Stramondo. 2017. “Earthquake Damage Mapping by Using Remotely Sensed Data: The Haiti
696 Case Study.” *Journal of Applied Remote Sensing*. https://doi.org/10.1117/1.JRS.11.016042.

697 Saito, Keiko, Robin Spence, Edmund Booth, Gopal Madabhushi, Ron Eguchi, and Stuart Gill. 2010.
698 “Damage Assessment of Port Au Prince Using Pictometry,” no. October.

699 Sedan, Olivier, Caterina Negulescu, Monique Terrier, Agathe Roulle, Thierry Winter, and Didier
700 Bertil. 2013. “Armagedom - A Tool for Seismic Risk Assessment Illustrated with Applications.”
701 *Journal of Earthquake Engineering* 17 (2): 253–81.
702 https://doi.org/10.1080/13632469.2012.726604.

703 Torres, Y, S Molina, S Martínez-Cuevas, M Navarro, J J Martínez-Díaz, B Benito, J J Galiana-
704 Merino, and D Belizaire. 2016. “A First Approach to Earthquake Damage Estimation in Haiti:
705 Advices to Minimize the Seismic Risk.” *Bulletin of Earthquake Engineering* 14 (1): 39–58.
706 https://doi.org/10.1007/s10518-015-9813-3.

707 UNITAR/UNOSAT, EC JRC and World Bank. 2010. “Joint Remote Sensing Damage Assessment.
708 Haiti Earthquake 12 January 2010.” http://www.unitar.org/unosat/haiti-earthquake-2010-remote-
709 sensing-based-building-damage-assessment-data.

710 USGS. 2017. “ShakeMap - M 7.0 - Haiti Region.” 2017.
711 https://earthquake.usgs.gov/earthquakes/eventpage/usp000h60h#shakemap.

712 Villar-Vega, Mabé, and Vitor Silva. 2017. “Assessment of Earthquake Damage Considering the
713 Characteristics of Past Events in South America.” *Soil Dynamics and Earthquake Engineering*
714 99: 86–96. https://doi.org/https://doi.org/10.1016/j.soildyn.2017.05.004.

715